Animal Reproduction Science 219 (2020) 106509

Contents lists available at ScienceDirect

Animal Reproduction Science

journal homepage: www.elsevier.com/locate/anireprosci

High-throughput sperm assay using label-free microscopy: morphometric comparison between different sperm structures of boar and stallion spermatozoa

Marcello Rubessa[a,b], Jean M. Feugang[e], Mikhail E. Kandel[d], Sierra Schreiber[a], Jade Hessee[a], Francesca Salerno[a], Sascha Meyers[a], Iwei Chu[f], Gabriel Popescu[c,d], Matthew B. Wheeler[a,b,c,*]

[a] Department of Animal Science, University of Illinois, Urbana-Champaign, IL 61801, USA
[b] Carl R. Woese Institute for Genomic Biology, Univ. of Illinois at Urbana-Champaign, USA
[c] Department of Bioengineering, University of Illinois, Urbana, Illinois 61801, USA
[d] Quantitative Light Imaging Laboratory, Department of Electrical and Computer Engineering, Beckman Institute of Advanced Science and Technology, USA
[e] Department of Animal and Dairy Sciences, Mississippi State University, Mississippi State, MS 39762, USA
[f] Institute for Imaging & Analytical Technologies, Mississippi State University, Mississippi State, MS 39762, USA

ARTICLE INFO

Keywords:
AFM
SLIM
Sperm
Swine
Stallion
Morphometry

ABSTRACT

The capacity for microscopic evaluation of sperm is useful for assisted reproductive technologies (ART), because this can allow for specific selection of sperm cells for *in vitro* fertilization (IVF). The objective of this study was to analyze the same sperm samples using two high-resolution methods: spatial light interference microscopy (SLIM) and atomic force microscopy (AFM) to determine if with one method there was more timely and different information obtained than the other. To address this objective, there was evaluation of sperm populations from boars and stallions. To the best of our knowledge, this is the first reported comparison when using AFM and high-sensitivity interferometric microscopy (such as SLIM) to evaluate spermatozoa. Results indicate that with the use of SLIM microscopy there is similar nanoscale sensitivity as with use of AFM while there is approximately 1,000 times greater throughput with use of SLIM. With SLIM, there is also allowace for the measurement of the dry mass (non-aqueous content) of spermatozoa, which may be a new label-free marker for sperm viability. In the second part of this study, there was analysis of two sperm populations. There were interesting correlations between the different compartments of the sperm and the dry mass in both boars and stallions. Furthermore, there was a correlation between the dry mass of the sperm head and the length and width of the acrosome in both boars and stallions. This correlation is positive in boars while it is negative in stallions.

1. Introduction

The capacity to use microscopic techniques to evaluate sperm with high-throughput procedures is useful for assisted reproductive

* Corresponding author: Biotechnology and Developmental Biology, Department of Animal Sciences, University of Illinois, 1207 West Gregory Drive, Urbana, IL 61801, USA.
E-mail address: mbwheele@illinois.edu (M.B. Wheeler).

https://doi.org/10.1016/j.anireprosci.2020.106509
Received 27 September 2019; Received in revised form 15 May 2020; Accepted 16 May 2020
Available online 23 May 2020
0378-4320/

technologies (ART) because this can allow for specific selection of sperm cells for *in vitro* fertilization (IVF). This utilization requires microscopy techniques that allow for a precise determination of high-quality spermatozoa while evaluating more variables than only motility and gross morphology. For example, assessing proper organelle functionality and cell membrane integrity, while simultaneously eliminating the need for labeling is highly desirable. When there is use of staining for sperm evaluations, these cells are no longer usable for IVF (Maree et al., 2010; Banaszewska et al., 2015; Kondracki et al., 2017).

Currently, there are several methods for imaging spermatozoa. The simplest is bright-field microscopy, though adequate observation requires staining of the cells and only general external morphology can be evaluated. Another method, with which there is the capacity for optimally outlining the edges of sperm cells is differential interference contrast [DIC] microscopy (Komiya et al., 2013). This methodology can be used to obtain only qualitative data because the acquired microscope image is not linearly related to the underlying structure of the sample. As a consequence, the image, when there is use of conventional microscopic techniques, cannot be used as a topographic map. This same issue is encountered when there is use of Hoffman modulation contrast (HMC) microscopy, an economically less expensive alternative to DIC microscopy, however, with a lesser capacity for precisely visualizing specific aspects of sperm structures (Shaked, 2016). Atomic force microscopy (AFM) can be conducted very efficiently for studying sperm, and the use of AFM has enabled for the discovery of the equatorial sub-segment in the head of spermatozoa from *Artiodactyla* (Ellis et al., 2002). The AFM procedures can be used for the measurement of the sperm head dimensions with the intact acrosome (Saeki et al., 2005). Besides allowing for more precise assessments of the characteristics of the sperm membrane, the information obtained with use of the AFM can be utilized for practical applications. In one study, there was the use of AFM to ascertain the effect of a male contraceptive on human sperm (Kumar et al., 2006), while in another study there was an investigation using AFM of whether there could be detection of important morphological differences between X- and Y-containing spermatozoa to improve current sperm sorting techniques (Carvalho et al., 2013). Even with the use of AFM to analyze various morphological characteristics, there has been no use of quantitative imaging modalities to evaluate conventional variables that are routinely used for quality assessments of boar and stallion spermatozoa. Quantitative image analysis of various sperm variables is important for determining what is an acceptable sperm cell when there is use of ART and may allow for development of new procedures that can be used for this analysis. In a previous study, there was measurement of sperm dimensions including the spermatozoa head, midpiece lengths and widths, as well as the principal piece, from 284 species using projection light microscopy techniques with Nigrosin-Eosin-staining of air-dried sperm (Cummins and Woodall, 1985). While AFM is a valuable research technique, the extremely low-throughput when there is evaluation of sperm is a major impediment for clinical utilization of this technique (Wang et al., 2011).

Quantitative phase imaging (QPI) (Popescu, 2011) is an emerging label-free imaging modality, which is valuable for several biomedical applications (Park et al., 2018). The QPI technique allows for combining of interferometric microscopy and holography approaches to yield quantitative maps of optical pathlength shifts in the specimen being evaluated. These pathlength maps can be easily converted into dry mass density distributions for evaluation of cellular structures (Miccio et al., 2011; Caprio et al., 2015). Spatial light interference microscopy (SLIM) is an alternative microscopy system that allows for combining of Zernike phase contrast microscopy with phase-shifting interferometry techniques. As a result, SLIM is extremely stable over time, highly sensitive spatially, and the implementation of use of this technology can occur with the addition of accessory equipment to existing microscopes (Wang et al., 2011; Kim et al., 2014). With this method, there is the capacity for imaging unlabeled spermatozoa and utilization of SLIM has occurred for the study of the topography and refractometry of spermatozoa (Liu et al., 2018).

In the present study, there was analysis of the same samples utilizing two accurate methods: SLIM and AFM. There was comparison of results when there was use of these two methods of SLIM imaging with a more conventional microscopy technique, focusing on four morphological variables of boar and stallion sperm. Specifically, there was assessment of the spermatozoa head length, head width, midpiece length, and tail length. To validate the methods, there was evaluation of spermatozoa of two different species, boar and stallion, with three subjects being assessed per species.

2. Materials and methods

2.1. Experimental design

2.1.1. Experiment 1

Semen from three boars and three stallions was spread onto a total of six slides (one for each animal). Using these slides, there was the initial comparison of the results when there were evaluations using the SLIM and AFM procedures. There subsequently was augmentation of these traditional morphological markers with information of the cellular dry mass of the segmented cellular compartments (head length, head width, midpiece length, and tail length). The dry mass quantitation is only possible with use of SLIM. From each slide, there was evaluation of 100 sperm using the SLIM and 20 sperm using the AFM procedures, for a total of 300 and 60 evaluations for boars and stallions.

2.1.2. Experiment 2

In the second experiment, there was examination of one slide from each of three boars and three stallions using the SLIM technology, totaling approximately 1,500 sperm per three boars and three stallions (~500 cells per animal). All standard variables were measured: head (length and width), acrosome (length and width) midpiece (length), tail (length) in μm. Furthermore, using the SLIM technology there was evaluation of sperm head and midpiece dry mass in picograms (pg).

2.2. Sample (semen) collection and preparation

Semen samples were collected from reproductively mature boars (n = 3) and stallions (n = 3) at different locations. Freshly extended boar semen was purchased from a commercial boar stud (Prestage Farms, West Point, MS), while stallion semen was collected (using artificial vagina) and extended at the Animal Research Facilities of Mississippi State University. All sperm samples were obtained, with consideration of the IACUC (MSU#14-006) guidelines in place at each location. These samples were extended in appropriate diluents before transportation to the laboratory. Extended boar and stallion spermatozoa were then purified using centrifugation procedures through a discontinuous Percoll gradient (700 x g – 30 minutes) and washed with a PBS-PVP, pH7.2 (1 mg/ml) solution (250 x g – 5 minutes), as previously described (Feugang et al., 2011). Purified sperm samples were fixed with 4% paraformaldehyde (ThermoFisher Scientific, Waltham, MA, USA) at room temperature. After 30 to 60 minutes, paraformaldehyde-fixed spermatozoa were spread on microscope slides and air-dried. Subsequently, slides were immersed overnight in deionized water, air-dried, and stored at room temperature or 4 °C until morphological and topographical analyses using AFM or SLIM procedures.

2.3. Atomic Force Microscope (AFM)

All sample imaging was performed using a Multimode Atomic Force Microscope (Bruker; Santa Barbara, CA), mounted on a vibration-free table to ensure reproducibility. Samples were imaged in the air using a tip (Bruker) with a spring constant of 0.32 N/m. After optimization of feedback gains and scan speed (typically 1.0 Hz, 1 line/second), sperm images were obtained using a contact-mode AFM and morphological structures were processed using the NanoScope Analysis software by manual tracing of spermatozoa. A total of 60 spermatozoa were analyzed for both the boars and stallions, with the length of the head, midpiece and tail, as well as the head width being considered.

2.4. Spatial Light Interference Microscopy (SLIM)

To obtain a quantitative phase map, with nanoscale sensitivity (Kandel et al., 2017), there was upgrading of the phase-contrast microscope (Z1, PC2 40x/0.7NA, Zeiss) with a spatial-light interference microscopy module (CellVista SLIM Pro, Phi Optics, Inc). Briefly, with utilization of SLIM procedures, there was a phase rather than intensity map generated that was associated with a transparent specimen. The procedure for imaging the slides was similar to that previously described (Liu et al., 2018). The dry-mass was calculated as a scaled sum of the halo-corrected phase values for each selection process (ImageJ's Integrated Density measure, NIH, Bethesda, MD). A total of 300 spermatozoa were analyzed for boars and stallions (Experiment 1) and ~1,500 spermatozoa were analyzed for boars and stallions (Experiment 2), with the head (length and width), acrosome (length and width) midpiece (length), tail (length), head dry mass and midpiece dry mass being evaluated.

2.5. Image analysis

Images were manually segmented using the ROI feature in ImageJ. As previously described (Majeed et al., 2018), dry-mass was calculated as a scaled sum of the halo-corrected phase values for each selection process. Consistent with common selection criteria (Carvalho et al., 2013), there were analyses of all imaged spermatozoa that had intact acrosomes. The diagram of a sperm cell and location where measurements were taken are depicted in Fig. 1.

2.6. Statistical analysis

In Experiment 1, when there was comparison of the two systems, there was a Mann–Whitney U test performed. In Experiment 2, a Pearson correlations (two-tailed) analysis was conducted, because of the objective to evaluate the association between all the values for morphological variables. All the analyses were conducted using SPSS (SPSS version 25. IBM, New York). With both analyses, there were considered to be statistical significance when there was a $P > 0.01$. Normality of residuals was assessed and found to be normal using the Shapiro-Wilk test.

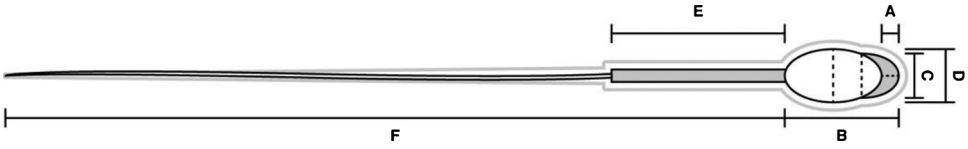

Fig. 1. Sperm cell diagram indicating specific measurements; Each lettered bar represents a sperm segment that was evaluated A & C = acrosome; B & D = sperm head; E = midpiece; F = tail including the midpiece.

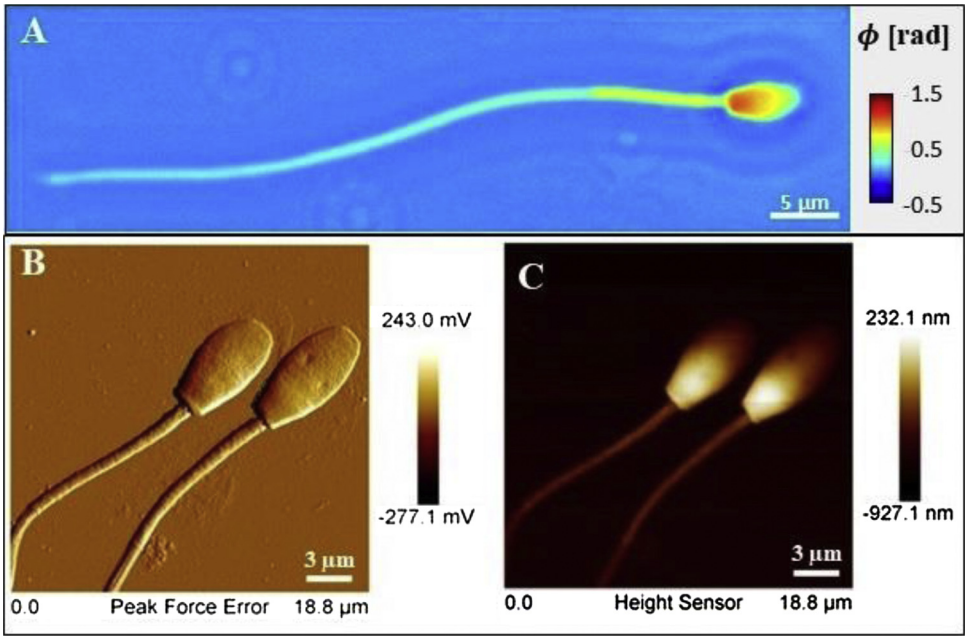

Fig. 2. Nanoscale images of stallion spermatozoa evaluated using SLIM (A) and AFM (B, C); Morphometry and topography of spermatozoa are generated with Peak Force images; Panel A, areas in red are denser than areas in blue; Panel B AFM power spectrum image indicating the roughness of the sperm surface; Panel C AFM height spectrum where the areas with white are thicker than areas with brown color; Head is clearly thicker where it attaches to the midpiece than in acrosomal area.

3. Results

3.1. Experiment 1: SLIM compared with AFM

The AFM images of stallion and boar spermatozoa are shown in Figs. 2 and 3, respectively. With both images, there are full (upper) and half (lower) lengths of spermatozoa that allowed for accurate measurements of sperm segments. The Peak Force Error images provide the means for evaluation of the nanoscale features of sperm morphometry and topography, while the Height Sensor

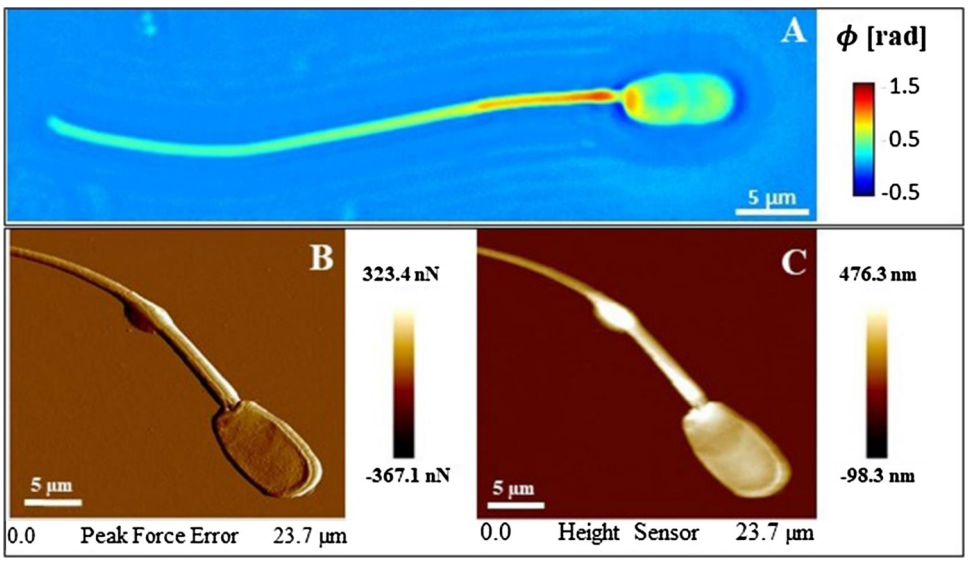

Fig. 3. Nanoscale images of boar spermatozoa acquired with SLIM (A) and AFM (B, C) Morphometry and topography of spermatozoa generated with Peak Force images; Panel A - areas in red are denser than the areas in blue; Panel B AFM power spectrum image indicating the roughness of the sperm surface; Panel C AFM height spectrum where areas in white are thicker than areas in brown color; Head is thicker where it attaches to the midpiece than in acrosomal area.

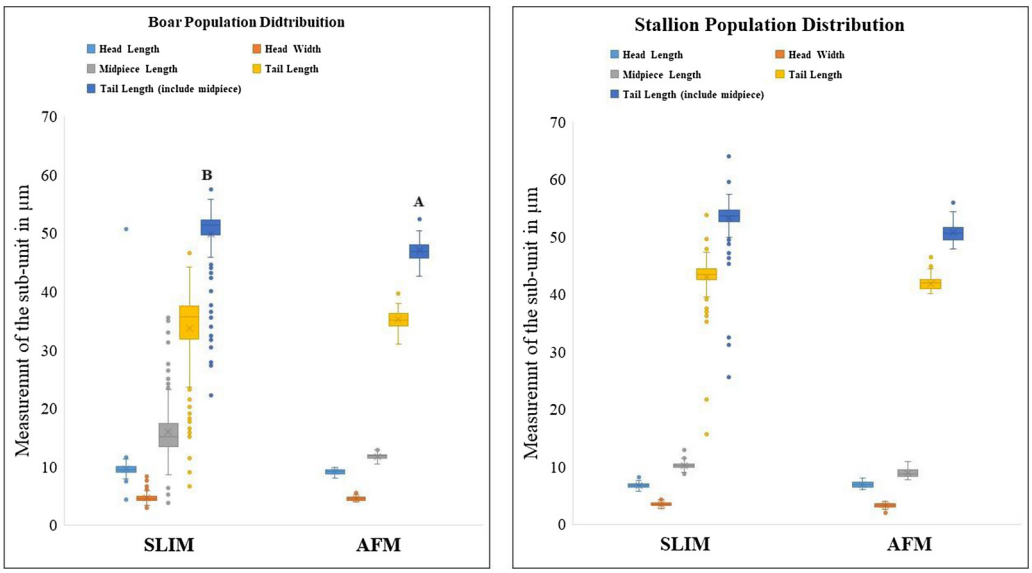

Fig. 4. Comparison of the two microscopy systems, SLIM and AFM: Population distribution of stallion and boar sperm morphometry; Y-axis measurements are in µm; $^{A, B}$ superscripts designate statistical differences between the measurements of the same morphometric sub-unit (i.e. Head Length or Head Width).

images provide for the capacity to conduct various measurements of each spermatozoon.

The data indicate there were no differences ($P > 0.05$) when there was use of the two imaging instruments (SLIM and AFM) with most measures being inconsistent less than 5% in mean value (Fig. 4, Supplemental Materials Table 1). The one inconsistency, however minor (< 20% difference; $P = 0.02$) was in sperm head lengths of boars.

Noteworthy is that with use of the AFM procedures there is greater resolution compared to use of widefield microscopy techniques, an image can be obtained using the SLIM procedures in less than a second, while the evaluation of a 4-megapixel AFM image on a state-of-the-art machine would take much longer due to its relatively slow scanning rate (~ six minutes/image in the current study). Furthermore, the reduced scanning area size when there was use of AFM (~150 x 150 µm) markedly limits the numbers of targeted spermatozoa, although the resulting images are of high quality to allow for various topographical and morphometric analyses.

3.2. Experiment 2: Analysis of boar and stallion spermatozoa populations

A total of 1,500 boar sperm were evaluated. In the supplemental materials (Table 2), there is reporting of the mean and the standard deviation for each variable. There was a positive correlation between the values for the measurements taken of the head (length and width) and acrosome (length and width). Furthermore, the values for spermatozoon midpiece length was positively correlated with the values for measurements of the head (length and width). The values for head dry mass were negatively correlated with those for the midpiece length and the head width, however, not with head length. The values for spermatozoon head dry mass were closely correlated with those for the acrosome length, tail length and midpiece dry mass. Furthermore, the values for spermatozoon head dry mass were positively correlated with those for the other variables evaluated. The values for spermatozoon midpiece dry mass were positively correlated with those for the length and width of the head and acrosome. The values for spermatozoon midpiece dry mass were positively correlated with those for the midpiece and tail length. All data for the correlation analysis are reported in Table 1 and are depicted in Supplemental Fig. 1.

In the second component of Experiment 2, there was a total of 1,593 sperm from three stallions evaluated. Means and the standard deviations of all measured variables are reported in Supplemental Table 2. There was a negative correlation between the values for spermatozoon midpiece dry mass, midpiece length, tail length, and head (length and width). The values for spermatozoon head length and width were positively correlated. There were also close negative correlations between values for the spermatozoon dry mass of the head and midpiece, as well as for values of the dry mass of the head and those for both acrosomal measurements (length and width). All the data for the correlation analyses are reported in Table 2 and are depicted in Supplemental Fig. 2. Also noteworthy, is with boar semen there are three sperm populations depicted in the two-dimensional dot plot (acrosome dimensions against dry mass) and with stallion sperm there are only two populations (Supplemental Figs. 1 and 2).

4. Discussion

The relatively few males that produce viable embryos when used for ART in livestock as well as relatively high incidence of human male factor infertility may suggest a need for examining new ways of evaluating male gametes. One new and exciting

Table 1
Pearson Correlation between values for boar sperm head length, head width, acrosome length, acrosome width midpiece (midpiece) length, tail length (midpiece included) and cell dry mass of the head and midpiece (pg)

		Head Length	Head Width	Acrosome Length	Acrosome Width	Midpiece Length	Tail Length (include midpiece)	Cell Dry Mass Midpiece	Cell Dry Mass Head
Head Length	Pearson Correlation	1	.132**	.307**	.195**	.203**	0.022	0.038	0.026
Head Width	Pearson Correlation	.132**	1	0.008	.131**	.182**	0.020	.068**	-.109**
Acrosome Length	Pearson Correlation	.307**	0.008	1	.696**	.071**	-.094**	0.029	.533**
Acrosome Width	Pearson Correlation	.195**	.131**	.696**	1	-.084**	−0.020	.086**	.530**
Midpiece Length	Pearson Correlation	.203**	.182**	.071**	-.084**	1	.166**	.307**	-.054*
Tail Length (include midpiece)	Pearson Correlation	0.022	0.020	-.094**	−0.020	.166**	1	.607**	.454**
Cell Dry Mass Midpiece (pg)	Pearson Correlation	0.038	.068**	0.029	.086**	.307**	.607**	1	.625**
Cell Dry Mass Head (pg)	Pearson Correlation	0.026	-.109**	.533**	.530**	-.054*	.454**	.625**	1

*Correlation $P \leq 0.05$ level (2-tailed); **Correlation $P \leq 0.01$ (2-tailed)

Table 2
Pearson Correlation between values for stallion sperm head length, head width, acrosome length, acrosome width midpiece (midpiece), tail length (midpiece included) and cell dry mass of head and midpiece (pg)

		Head Length	Head Width	Acrosome Length	Acrosome Width	Midpiece Length	Tail Length (include midpiece)	Cell Dry Mass Midpiece	Cell Dry Mass Head
Head Length	Pearson Correlation	1	.408**	.207**	0.003	.127**	.145**	-.132**	.163**
Head Width	Pearson Correlation	.408**	1	-.061*	−0.033	.061*	.118**	-.552**	.359**
Acrosome Length	Pearson Correlation	.207**	-.061*	1	.400**	−0.048	.051*	.464**	-.523**
Acrosome Width	Pearson Correlation	0.003	−0.033	.400**	1	-.156**	−0.042	.254**	-.568**
Midpiece Length	Pearson Correlation	.127**	.061*	−0.048	-.156**	1	.200**	-.159**	.207**
Tail Length (include midpiece)	Pearson Correlation	.145**	.118**	.051*	−0.042	.200**	1	−0.029	.101**
Cell Dry Mass Midpiece (pg)	Pearson Correlation	-.132**	-.552**	.464**	.254**	-.159**	−0.029	1	-.515**
Cell Dry Mass Head (pg)	Pearson Correlation	.163**	.359**	-.523**	-.568**	.207**	.101**	-.515**	1

*Correlation $P \leq 0.05$ (2-tailed); **Correlation $P \leq 0.01$ (2-tailed)

possibility is label-free imaging of sperm cells. Ferrara et al. analyzed bull sperm using the label-free methods utilizing Rahman spectroscopy and digital holography in an attempt to ascertain differences between the X-sperm and Y-sperm populations (Ferrara et al., 2015). Using these methods, there were not any detectable morphological differences between the two populations. The AFM procedures have previously been used to evaluate spermatozoa (Allen et al., 1995; Kumar et al., 2005b). Furthermore, using AFM, there was found to be a correlation between the values for head shape and chromatin condensation (Kumar et al., 2005a; Ma et al., 2019). To our knowledge, the present study is the first in which there was a comparison of findings with the use of high sensitivity AFM, with SLIM, a label-free quantitative imaging microscope that combines Zernike phase contrast microscopy with phase shifting interferometry, to evaluate spermatozoa. There is considerable interest in the development of label-free microscopy because with this technique there can be evaluation of biological samples without modifications, introduction of dyes or pretreating the samples. In a previous study, Kondracki et al. (2017) compared two different staining methods and the results indicated how shape and size of the boar spermatozoon changes as a result of staining (Kondracki et al., 2017). This is not an isolated case because in other studies results indicated that staining results in changes in the values for spermatozoa variables of other species, including humans (Maree et al., 2010; Banaszewska et al., 2015). Another advantage of label-free SLIM microscopy is the relatively shorter period of time that is required to conduct these procedures as compared with the electronic microscopy or AFM to complete the analysis of sperm samples (Wang et al., 2011). Results of the present study indicate there is consistency between data obtained using AFM and quantitative phase imaging procedures utilizing the SLIM. The only difference between the values with use of these two procedures are those for boar head length, which is attributed to observational bias, because the two categories were evaluated by different research groups. With use of these two imaging modalities, there is normally measurement of samples within a fraction of a nanometer (Wang et al., 2011). The SLIM imaging technology is different from AFM imaging in that SLIM is non-contact, parallel to the sample and is faster, "by greater than three orders of magnitude" (Wang et al., 2011). The SLIM system can be used to measure areas of "$\sim 75 \times 100\ \mu m^2$ in 0.5 s while the AFM is only able to measure an area of 10 × 10 μm2 in 21 minutes" (Wang et al., 2011).

Due to the comparability of the two technologies, with the present study the goal was to characterize the sperm population of boars and stallions utilizing the SLIM technology. Values for boar sperm evaluated using SLIM were similar (on a decimal scale) to values determined by other groups (Cummins and Woodall, 1985; Kondracki et al., 2017). To the best of our knowledge, this is the first study in which there was quantitation of the dry mass of the head and midpiece of mammalian spermatozoa. There were close correlations between the values for variables examined. One interesting observation was that there was a close correlation between the values for dry mass of the head and those for the dry mass of the midpiece. Furthermore, as expected the values for dry mass of the head were correlated with the values for the other variables examined, such as midpiece dry mass and length, and values for all sperm head variables, including the acrosome. Interestingly, there were not any correlations between values for sperm length and dry mass.

Similar to values for the boar sperm variables, those values determined using SLIM in stallions were comparable to those previously reported (Cummins and Woodall, 1985; Gravance et al., 1996). Interestingly, there was a correlation between values for head dry mass and those for all other measured variables. Curiously, there was not a close correlation between the values for head sizes and those for the head dry mass in either sperm of boars or stallions. Furthermore, there was a close correlation between the values for acrosome sizes and the dry mass of boar sperm. In stallion sperm, there was a negative correlation between the two dry masses (head and midpiece). This result is in contrast to the findings with boar sperm, where there was a close positive correlation between values for head and midpiece dry mass. Another interesting difference in boar and stallion sperm is the association between values for the midpiece mass and head width. While in the stallion there is a close negative correlation, in the boar there is a positive correlation between values for these two variables. There was a linear correlation between the values for measurements of length and width of the spermatozoon head and length and width of the acrosome.

The reasons for the differences between the morphometric correlations between the boar and the stallion sperm in the present study are not clear. Certainly, species differences may account for a portion of these results. The heterogeneity of sperm in individual ejaculates may also affect these differences. Heterogeneity of spermatozoa, however, is important to ensure an increased fertilization potential in the female tract (Garcia-Vazquez et al., 2016). The use of inbred lines of boars from a commercial source and stallions from a single breed may have exacerbated the differences observed in the present study.

In the present study, there was not an evaluation of fertility of the test subjects but there has been a review focused on the importance of sperm morphology/morphometry to sperm transport in the female reproductive tract and fertilization (Garcia-Vazquez et al., 2016). It was suggested that while sperm dimensions of most domestic farm animals were similar, this decreased variation may be due to reduced competition between males which has resulted from the selection of high genetic merit sires (Garcia-Vazquez et al., 2016). In the horse, it has been reported that the specific characteristics of the sperm depend on the social environment and the presence or absence of other stallions and mares (Burger et al., 2015). The repeated collection of the stallion semen using an artificial vagina may have affected the values for some of these variables in the present study. The capacity of sperm to be transported into the upper portions of the female tract is an important aspect of fertilizing capacity. Garcia-Vazquez et al. (2015) reported that boar sperm with small heads and tails were the first to be observed in the backflow after uterine- or cervical-site artificial insemination. In stallions, there are larger sperm head lengths, areas, and sperm head perimeters that are associated with subfertile males as compared with highly fertile males (Gravance et al., 1996; Casey et al., 1997). Similarly in boars, greater fertility was associated with a lesser sperm head area and length and larger width and width/length ratio values (Hirai et al., 2001). Using inbred boars from high fertility commercial lines may have affected results in the present study. While the findings from assessing these variables are interesting to consider as causative factors related to sperm fertilizing capacity, the simple explanation for the differences in the correlations between values for boar and stallion sperm is that there was not examination of enough animals. In the present study, there was analysis of hundreds of sperm using the SLIM and AFM technologies but there is likely a need to examine many more individual animals to determine if these differences in correlations between the spermatozoa of boars and stallions can be verified in future

studies.

The present results illustrate that with use of SLIM microscopy there is a similar sensitivity as with use of AFM while being 10,000 times faster for conducting the procedures. Furthermore, SLIM allows for measurement of the dry mass of the spermatozoa. It is believed that this variable could be used as a marker for high-quality sperm because sperm mass will change when the spermatozoa include vacuoles or are incomplete. Furthermore, because there was correlation determinations between the values for acrosome and dry mass, this variable could be used to evaluate the acrosome reaction as well. It is important to highlight that in results from the present study the correlation was positive in the boar while being negative in the stallion.

5. Conclusion

The results from the analysis of boar and stallion sperm populations indicate there are aspects of the morphometrics of this particular cell that might be important for evaluating spermatozoon fertilizing capacity. Because there was only analyses of spermatozoa that did not have malformations (vacuoles, cytoplasmic droplets, absent acrosomes), these variables could be used as standards for evaluation of sperm quality in the future. These results combined with those from previous research, where there were assessment of dry, fixed sperm cells or sperm in fluid (Liu et al., 2018) indicate SLIM microscopy may be a valuable technique for evaluation of sperm. Furthermore, unlike AFM, SLIM is a high-throughput machine that can easily be adapted for conducting IVF and ICSI procedures. This is especially the situation with the ICSI procedure, where the variables for the selection of the spermatozoa are limited, the utilization of SLIM in association with the micromanipulator could lead to improvements in the success rate when conducting ICSI. Consequently, further research needs to be conducted to compare the findings in the present study with results from studies where there are evaluations of defective spermatozoa, as well as to compare fertilization and pregnancy rates using sperm that are characterized to have desirable values for variables assessed in the present study using SLIM.

Declaration of Competing Interest

G.P has a financial interest in Phi Optics, Inc., a company developing quantitative phase imaging technology for materials and life science applications.

Funding sources

This research was partially supported by the USDA Multistate Project W-4171 (MBW, JMF), the Ross Foundation (MBW, MR), < GS3 > USDA-ARS, Biophotonic Initiative < /GS3 > grant < GN3 > #58-6402-3-018 < /GN3 > (JMF) and by National Science Foundation grant NRT-UtB 1735252 (MEK).

Author contributions

MR, MK, JMF and MBW designed the experiment. MR and JMF prepared the samples. JMF and IC performed the AFM imaging. SS and SM performed the SLIM imaging SS performed manual segmentation on SLIM images. MR and MK performed data analysis. GP and MBW supervised the work. MR and MBW wrote the manuscript.

Acknowledgments

The authors would like to thank Molly Sermersheim for carefully reading the manuscript. This paper is dedicated to Dr. Richard Arthur Fayrer-Hosken, a dedicated scientist, an animal lover, and a good friend! We will miss him dearly!

Appendix A. Supplementary data

Supplementary material related to this article can be found, in the online version, at doi:https://doi.org/10.1016/j.anireprosci.2020.106509.

References

Allen, M.J., Bradbury, E.M., Balhorn, R., 1995. The natural subcellular surface structure of the bovine sperm cell. J. Struct. Biol. 114, 197–208.
Banaszewska, D., Andraszek, K., Czubaszek, M., Biesiada-Drzazga, B., 2015. The effect of selected staining techniques on bull sperm morphometry. Anim Reprod Sci 159, 17–24.
Burger, D., Dolivo, G., Wedekind, C., 2015. Ejaculate Characteristics Depend on Social Environment in the Horse (Equus caballus). PLOS ONE 10, e0143185.
Caprio, G., Ferrara, M.A., Miccio, L., Merola, F., Memmolo, P., Ferraro, P., Coppola, G., 2015. Holographic imaging of unlabelled sperm cells for semen analysis: a review. Journal of biophotonics 8, 779–789.
Carvalho, J.O., Silva, L.P., Sartori, R., Dode, M.A., 2013. Nanoscale differences in the shape and size of X and Y chromosome-bearing bovine sperm heads assessed by atomic force microscopy. PloS one 8, e59387.
Casey, P.J., Gravance, C.G., Davis, R.O., Chabot, D.D., Liu, I.K.M., 1997. Morphometric differences in sperm head dimensions of fertile and subfertile stallions. Theriogenology 47, 575–582.
Cummins, J.M., Woodall, P.F., 1985. On mammalian sperm dimensions. Journal of reproduction and fertility 75, 153–175.
Ellis, D.J., Shadan, S., James, P.S., Henderson, R.M., Edwardson, J.M., Hutchings, A., Jones, R., 2002. Post-testicular development of a novel membrane substructure

within the equatorial segment of ram, bull, boar, and goat spermatozoa as viewed by atomic force microscopy. Journal of structural biology 138, 187–198.
Ferrara, M.A., Di Caprio, G., Manago, S., De Angelis, A., Sirleto, L., Coppola, G., De Luca, A.C., 2015. Label-free imaging and biochemical characterization of bovine sperm cells. Biosensors 5, 141–157.
Feugang, J.M., Greene, J.M., Willard, S.T., Ryan, P.L., 2011. In vitro effects of relaxin on gene expression in porcine cumulus-oocyte complexes and developing embryos. Reproductive biology and endocrinology: RB&E 9, 15.
Garcia-Vazquez, F., Gadea, J., Matas, C., Holt, W., 2016. Importance of sperm morphology during sperm transport and fertilization in mammals. Asian Journal of Andrology 18, 844–850.
Gravance, C.G., Liu, I.K., Davis, R.O., Hughes, J.P., Casey, P.J., 1996. Quantification of normal head morphometry of stallion spermatozoa. J Reprod Fertil 108, 41–46.
Hirai, M., Boersma, A., Hoeflich, A., Wolf, E., FÖLl, J., AumÜLler, R., Braun, J., 2001. Objectively Measured Sperm Motility and Sperm Head Morphometry in Boars (Sus scrofa): Relation to Fertility and Seminal Plasma Growth Factors. Journal of Andrology 22, 104–110.
Kandel, M.E., Teng, K.W., Selvin, P.R., Popescu, G., 2017. Label-Free Imaging of Single Microtubule Dynamics Using Spatial Light Interference Microscopy. ACS Nano 11, 647–655.
Kim, T., Zhou, R.J., Mir, M., Babacan, S.D., Carney, P.S., Goddard, L.L., Popescu, G., 2014. White-light diffraction tomography of unlabeled live cells. Nature Photonics 8, 256–263.
Komiya, A., Watanabe, A., Kato, T., Kawauchi, Y., Fuse, H., 2013. Observation of spermatozoa by a high-magnification microscope. Reproductive medicine and biology 13, 21–28.
Kondracki, S., Wysokinska, A., Kania, M., Gorski, K., 2017. Application of Two Staining Methods for Sperm Morphometric Evaluation in Domestic Pigs. J Vet Res 61, 345–349.
Kumar, S., Chaudhury, K., Sen, P., Guha, S.K., 2005a. Atomic force microscopy: a powerful tool for high-resolution imaging of spermatozoa. Journal of nanobiotechnology 3, 9.
Kumar, S., Chaudhury, K., Sen, P., Guha, S.K., 2005b. Atomic force microscopy: A powerful tool for high-resolution imaging of spermatozoa. J. Nanobiotechnol. 3, 3–9.
Kumar, S., Chaudhury, K., Sen, P., Guha, S.K., 2006. Topological alterations in human spermatozoa associated with the polyelectrolytic effect of RISUG®. Micron 37, 526–532.
Liu, L., Kandel, M.E., Rubessa, M., Schreiber, S., Wheeler, M.B., Popescu, G., 2018. Topography and refractometry of sperm cells using spatial light interference microscopy. Journal of biomedical optics 23, 1–6.
Ma, Y., Xie, N., Li, Y., Zhang, B., Xie, D., Zhang, W., Li, Q., Yu, H., Zhang, Q., Ni, Y., Xie, X., 2019. Teratozoospermia with amorphous sperm head associate with abnormal chromatin condensation in a Chinese family. Syst Biol Reprod Med 65, 61–70.
Majeed, H., Ma, L., Lee, Y.J., Kandel, M., Min, E., Jung, W., Best-Popescu, C., Popescu, G., 2018. Magnified Image Spatial Spectrum (MISS) microscopy for nanometer and millisecond scale label-free imaging. Optics express 26, 5423–5440.
Maree, L., du Plessis, S.S., Menkveld, R., van der Horst, G., 2010. Morphometric dimensions of the human sperm head depend on the staining method used. Hum Reprod 25, 1369–1382.
Miccio, L., Finizio, A., Memmolo, P., Paturzo, M., Merola, F., Coppola, G., Di Caprio, G., Gioffre, M., Puglisi, R., Balduzzi, D., Galli, A., Ferraro, P., 2011. Detection and visualization improvement of Spermatozoa cells by Digital Holography. Proc Spie 8089.
Park, Y., Depeursinge, C., Popescu, G., 2018. Quantitative phase imaging in biomedicine. Nature Photonics 12, 578.
Popescu, G., 2011. Quantitative phase imaging of cells and tissues. McGraw-Hill, New York.
Saeki, K., Sumitomo, N., Nagata, Y., Kato, N., Hosoi, Y., Matsumoto, K., Iritani, A., 2005. Fine surface structure of bovine acrosome-intact and reacted spermatozoa observed by atomic force microscopy. The Journal of reproduction and development 51, 293–298.
Shaked, N.T., 2016. Label-Free Quantitative Imaging of Sperm for In-Vitro Fertilization Using Interferometric Phase MicroscopyIVF, IMSI, ICSI, IPM, Holography, Imaging, Sperm. Journal of Fertilization: In Vitro - IVF-Worldwide, Reproductive Medicine, Genetics & Stem Cell Biology 4.
Wang, Z., Millet, L., Mir, M., Ding, H., Unarunotai, S., Rogers, J., Gillette, M.U., Popescu, G., 2011. Spatial light interference microscopy (SLIM). Optics express 19, 1016–1026.